Bull. Mater. Sci., Vol. 25, No. 5, October 2002, pp. 419–429. © Indian Academy of Sciences.

Preliminary *in vitro* and *in vivo* characterizations of a sol–gel derived bioactive glass–ceramic system

S ABIRAMAN, H K VARMA, T V KUMARI, P R UMASHANKAR and ANNIE JOHN*

Biomedical Technology Wing, Sree Chitra Tirunal Institute for Medical Sciences and Technology, Poojapura, Thiruvananthapuram 695 012, India

MS received 27 November 2001; revised 5 August 2002

Abstract. This study investigates quantitatively and qualitatively the sol–gel derived bioactive glass–ceramic system (BGS)—apatite–wollastonite (AW) type granules in the size range of 0·5–1 mm, as an effective graft material for bone augmentation and restoration. Scanning electron micrographs (SEM) of the sintered granules revealed the rough material surface with micropores in the range 10–30 µm. X-ray diffraction (XRD) pattern of the granules revealed the presence of crystalline phases of the hydroxyapatite and wollastonite, and the functional groups of the silicate and phosphates were identified by Fourier transform infrared spectroscopy (FT-IR). The *in vitro* cell culture studies with L929 mouse fibroblast cell line showed very few cells adhered on the BGS disc after 24 h. This could be due to the highly reactive surface of the disc concomitant with the crystallization but not due to the cytotoxicity of the material, since the cellular viability (MTT assay) with the material was 80%. Cytotoxicity and cytocompatibility studies proved that the material was non-toxic and biocompatible. After 12 weeks of implantation of the BGS granules in the tibia bone of New Zealand white rabbits, the granules were found to be well osteointegrated, as observed in the radiographs. Angiogram with barium sulphate and Indian ink after 12 weeks showed the presence of microcapillaries in the vicinity of the implant site implicating high vascularity. Gross observation of the implant site did not show any inflammation or necrosis. SEM of the implanted site after 24 weeks revealed good osteointegration of the material with the newly formed bone and host bone. New bone was also observed within the material, which was degrading. Histological evaluation of the bone healing with the BGS granules in the tibial defect at all time intervals was without inflammation or fibrous tissue encapsulation. After 2 weeks the new bone was observed as a trabeculae network around the granules, and by 6 weeks the defect was completely closed with immature woven bone. By 12 weeks mature woven bone was observed, and new immature woven bone was seen within the cracks of the granules. After 24 weeks the defect was completely healed with lamellar bone and the size of the granules decreased. Histomorphometrically the area percentage of new bone formed was 67·77% after 12 weeks and 63·37% after 24 weeks. Less bone formation after 24 weeks was due to an increased implant surface area contributed by the material degradation and active bone remodeling. The osteostimulative and osteoconductive potential of the BGS granules was established by tetracycline labelling of the mineralizing areas by 2 and 6 weeks. This sol–gel derived BGS granules proved to be bioactive and resorbable which in turn encouraged active bone formation.

Keywords. Bioactive glass–ceramic; fibroblast cells; tibia bone; osteogenesis.

1. Introduction

Local defects in bone as a result of disease or trauma are frequently restored by bone graft substitutes. Historical records from implantation of natural minerals and gemstones goes far back to the period 600–800 A.D. (Epstein 1989), followed by ivory, inert metals, and bone products (Ludwigson 1964). Autografts being the most preferred, has problems like limited supply and morbidity. Again, allografts have the high risk of transmission of infections, fracture and non-union, high cost and storage, in tissue replacements for bony skeletal defects. Over the past decade, we have come across various artificial materials such as metals, polymers and ceramics, which are developed, as bone substitutes to overcome the common problems associated with natural bone grafts in reconstructive surgery. It is now widely understood that synthetic bone grafts that possess the bioactive property, would aid in regaining shape and function of the defective bone by serving as a scaffold for bone growth and can contribute to the healing process.

Bioglass and apatite wollastonite (AW) glass–ceramic of different forms and sizes, either dense or porous are synthesized and are widely used as substitutes for bone augmentation and restoration, in orthopaedic, dental and maxillofacial surgery (Hench and Paschall 1973; Hench and Wilson 1984; Hench 1988; Hench 1991a, 1994;

*Author for correspondence

Hench and West 1996; Ratner *et al* 1996) and to assist in tissue engineering (Bruder *et al* 1998). Such materials are bioactive, biocompatible, mechanically stable, biodegradable and favour osseointegration (Nakamura *et al* 1985; Holmes *et al* 1988; Hupp and McKenna 1988; Hench 1991b; Hench and Andersson 1993; Neo *et al* 1993; Kitsugi *et al* 1995; Oonishi *et al* 2000). The high bioactivity of AW glass–ceramic might be attributed to the high rate of formation of the apatite layer on AW glass–ceramic (Kokubo *et al* 1989). Calcium phosphate rich layer or apatite layer has also been observed for Bioglass® type glass (Hench and Clark 1981) and Ceravital® type glass ceramic (Ohtsuki *et al* 1991). In addition to all the above requirements, an ideal bioactive material is simultaneously expected to have an intimate apposition with both bone/soft connective tissues at the interface (Van Blitterswijk *et al* 1985; Hench 1994; Hench and West 1996). In contrast to the osteoconductive hydroxyapatite and AW glass–ceramic (Hench 1994; Hench and West 1996), certain compositions of bioactive glasses accelerate bone proliferation by a process called osteoproduction (where a bioactive surface is colonized by osteogenic stem cells free in the defect environment as a result of surgical intervention) which is due to both intracellular (owing to release of soluble silica) and extracellular factors (chemisorption of bone growth proteins) (Wilson and Low 1992). So it is quite obvious that the material surface/cell interaction is the key issue to accomplish the bone bonding.

This study characterizes the physical properties such as the crystallinity and surface morphology of the sol–gel derived bioactive glass–ceramic system, synthesized in-house. Furthermore, they are evaluated for their biocompatibility *in vitro* using L929 fibroblast cells and subsequently for their respective osseous regeneration and healing *in vivo* in a rabbit tibial-defect model.

2. Experimental

2.1 *Material*

The forms of the material used in this study were bioactive glass–ceramic system (BGS) – (SiO_2/CaO/P_2O_5/MgO system) granules and BGS disc, synthesized and developed in-house as part of the bioceramics programme for bone substitute materials.

2.1a *Preparation of bioactive glass–ceramic granules and disc*: The synthesized calcium phosphate based glass–ceramic (BGS) has the chemical composition: CaO 45%, SiO_2 34%, P_2O_5 16%, MgO 5%.

The material was synthesized by a sol–gel method involving silicon alkoxide, calcium nitrate and phosphorous pentoxide. A uniform sol was made by dissolving calcium nitrate and phosphorous pentoxide in deionized distilled water and mixed and refluxed with alkoxide solution. The clear solution thus obtained was allowed to gel at room temperature for 24 h to get a transparent body. This transparent gel was slowly heated to 1200–1300°C for sintering. The sintered gel was crushed using an agate mortar and sieved through a 0·5–1 mm mesh and this fraction of granules were collected.

The sintered BGS disc was prepared by compressing the gel powder (calcined at 600°C for 2 h) to the disc form of 10 mm diameter and 3 mm thick pellets, and sintered at 1200°C for 2 h. The bulk density of BGS was around 80–85% with intragranular porosities in the range 10–30 μm.

The granules and discs thus obtained were thoroughly cleaned in acetone and deionized distilled water in an ultrasonicator. Subsequently they were sterilized in an autoclave, prior to *in vitro* and *in vivo* evaluations.

2.2 *Characterization of the phase purity and crystallinity of the sol–gel BGS*

2.2a *Scanning electron microscope (SEM)*: The granules were gold coated in an ion sputter (E101-Hitachi) and examined for their size and microstructure (pore size, shape and interconnectivity) in SEM (S2400-Hitachi).

2.2b *X-ray diffraction analysis (XRD)*: XRD pattern of BGS was recorded in a diffractometer (Siemens 2000), performed at 40 kV and 30 mA, using a step size of 0·100°, scan rate of 2q per min and a scan range between 20° and 40° 2q in flat plate geometry with K-Alpha 1 radiation, for phase purity and crystallinity.

2.2c *Fourier transform infrared spectroscopy (FTIR)*: The IR spectrum of synthetic BGS was recorded using a Nicolet Impact 410 FT-IR spectroscopy, using the KBr pellet technique. Samples were mixed with KBr powder in a weight ratio of 1 : 100 mg and pressed into pellets and analysed at a resolution of four wave numbers, operating from 4000 to 400 cm^{-1}.

2.3 *In vitro studies*

An *in vitro* model comprising of L929 mouse fibroblast cell line (National Centre for Cell Sciences, Pune, India) was used to test the toxicity of BGS granules.

2.3a *Direct contact with materials*: Cells (1×10^3 cells/well) were seeded in 24-well tissue culture polystyrene plates enriched in Dulbecco's minimum essential medium (DMEM) with Earl's salt (Highmedia, Pune, India), supplemented with 10% foetal calf serum (FCS), 100 units and 100 mg/ml, respectively of penicillin and streptomycin and incubated at 37°C for 24 h and 5% CO_2 air. When the cells attained confluency, the cleaned and

sterilized granules were placed in direct contact with the cells in the wells and left for 24 h under the same condition. Thereafter the cells were observed under phase contrast microscope for any change in morphology or any other cytopathic effect when compared with negative and positive controls.

2.3b *Cell viability (MTT assay)*: Known weight of the granules were placed in DMEM with Earl's salt for 24 h, after which the material extract was taken. Known volume of the extract was then placed in contact with the confluent layer of fibroblast cells in 96-well Tissue Culture Plate (Nunc) enriched with 1 ml of DMEM with Earl's salt supplemented with 10% FCS and 100 units and 100 mg/ml, respectively of penicillin and streptomycin. Cultures were maintained in a humidified atmosphere of 95% air, 5% CO_2, at 37°C. To the control group of cells no extract was added. After contact with the material extract for 24 h, cells were washed with phosphate buffer and allowed to react with MTT dye solution (3-4,5-dimethylthiazol-2yl)-2,5-diphenyl-tetrazolium bromide). MTT assay is a common assay for testing cellular viability based on the reductive cleavage of yellow tetrazolium salt to a purple formazon compound by the dehydrogenase activity of intact mitochondria. Consequently, this conversion only occurs in living cells. Plates were incubated at 37°C for 4 h for the cells to react with the dye. MTT solutions were removed and *n*-propanol was added to all the wells. The plates were slightly shaken for 10 min to ensure crystal dissolution and absorbance was measured in a Multiplate Reader (Biotek) at the wavelength of 570 nm. The percentage of cells with the material extract was determined by comparing their respective absorbance with that of the control cells.

2.3c *Cytocompatibility*: To visualize cell adhesion on the surface of the material, cells (1×10^3 cells) were seeded on the surface of conditioned (disc soaked in DMEM with Earl's salt for 24 h) bioactive glass–ceramic disc (10 × 3 mm size). They were maintained in the same culture medium for 48 h. Thereafter the disc with the cells were fixed in 3% glutaraldehyde, post-fixed in 1% osmium tetroxide, dehydrated in acetone, critical point dried (HCP2-Hitachi), gold coated in an ion sputter (E101-Hitachi) and viewed in SEM (S2400 Hitachi).

2.4 *In vivo studies*

2.4a *Animal model*: Eight New Zealand white male rabbits (2 to 2·5 kg) were randomly assigned to two groups of four rabbits each. The transcortical bone-pin model for assessment of the *in vivo* bone response was adapted from the American Society for Testing of Materials (ASTM). Management of animal husbandry and postoperative care of the rabbits in the vivarium are standardized in-house, as per the guidelines of the Committee for the Purpose of Control and Supervision of Experiments (CPCSE).

BGS granules were implanted in the tibial defects (proximal and distal site) to evaluate the cortical bone response and to specifically assess the behaviour of the material in bone at consecutive time period of 2, 6, 12 and 24 weeks.

2.4b *Surgical procedure*: A 2 cm longitudinal incision was made in the muscle (*tibialis.m*) of the rabbit, exposing the tibia bone. The periosteum was incised and retracted using a periosteum elevator. A defect size of 2 mm diameter with a depth of ~ 1·5 mm was made using a surgical dental drill of 2 mm size at 2000 rpm, under constant irrigation of cold saline to avoid thermal necrosis and to remove the debris. The BGS granules were press fit into the defects using dental filler, and the periosteum, muscle and skin were sutured in layers.

2.4c *Post operative care*: The wound was dressed with neosporin and ampicillin and cloxicillin 50 mg/kg was given once daily for 5 postoperative days. Sutures were removed on the seventh day. During this period the animals were observed for any wound infection.

2.4d *Fluorescence labelling in bone*: To label the active zones of bone mineralization, one animal each at 2 and 6 weeks period was injected intramuscularly with tetracycline (25–50 mg/kg) at one and two weeks, respectively prior to sacrifice.

2.4e *Bone vasculature studies (angiogram)*: An attempt was made to study the neo-vascularization after implantation. Briefly, before sacrificing the animal at 12 weeks, barium sulphate and Indian ink were infused separately in one animal to study the vasculature status of the implanted site. Femoral artery and femoral vein cannulated and flushed the bloodline with one litre of heparinised ringer lactate. Once the outlet flow became clear of blood, 30% barium sulphate ($BaSO_4$) suspension (0·4–0·6 µm particle size) with Indian ink 140 ml + 500 ml ringer lactate was infused via a cardioplegia infusion set at 120–150 mm Hg and 15 min later 30% of $BaSO_4$ with 140 ml of Indian ink + 10% buffered formalin was flushed as above for 15 min (Plenk 1986). The whole leg with the cannulae *in situ* was kept in 10% buffered formalin for 3 days for fixation and then X-ray was taken. Thereafter, sections (3–4 mm in size) of the implant area were taken, decalcified in Von Ebner's decalcifying fluid (36% sodium chloride in concentrated hydrochloric acid), dehydrated in alcohol, embedded in polymethyl methacrylate (PMMA) and finally the X-ray radiograph was taken. The X-ray film was then captured in a CCD camera under the light microscope to observe clearly any blood capillaries at the implant site.

2.5 *Evaluation methods*

2.5a *Radiography*: Radiography of the bone-implant site in the tibia bone was taken after the implantation and before sacrifice, for all the groups using a Dental X-ray Unit (N Villa Sistemi Medicali-Model 83603).

2.5b *Histology*: Animals were euthanized at the specific period with high dosage of sodium thiopentone and the tibia bone was disarticulated from the anterior (Femur) and the posterior joints (metatarsal) and immediately fixed in 10% buffered formalin.

The bone was carefully cleaned of all attached muscles and cut perpendicular to the implant with a diamond blade in an Isomet (Beuhler) into 5 mm thick blocks with the ceramic implant. These blocks were immediately immersed in 10% phosphate-buffered formaldehyde. Cross-section of implant site was photographed. Fluorescence labelled bone samples were fixed in 70% ethyl alcohol. Thereafter, both the samples (labelled and unlabelled) were dehydrated in graded series of alcohol and embedded in PMMA. Thin sections were made using a diamond saw (Isomet, Beuhler) to a thickness of 100–200 μm and ground to 150 μm using the grinding machine (Beuhler). Following staining of the undecalcified sections with Stevenel's blue and counter stained with van Gieson picrofuschin (Gurr 1973), sections were examined with light microscopy and subjected to histomorphometric analysis. Unstained PMMA section was also gold coated in an ion sputter (E101-Hitachi) and observed in SEM (Hitachi S2400).

2.5c *Histomorphometric analysis (Optimas 6·1 version software)*: Histomorphometric analysis was performed to quantify the area of the new bone formed around the implant at 3 and 6 months postimplantation. For quantitative evaluation of the residual granules and the new bone formed, the images were captured through a charged coupled device (CCD) camera attached to the microscope in a 24-bit RGB mode and a frame width of 768/576 pixels. The images were calibrated and suitable thresholding was done to calculate the area percentage of new bone formed with respect to the bioactive glass–ceramic system granules. Student's *t*-test was done to compare the significance between the 3 months and 6 months implanted samples.

2.5d *Fluorescence microscopy*: Unstained fluorescence labelled PMMA polished sections of 100–150 μm thickness were viewed under the fluorescence microscopy (NIKON E600 Epifluorescent Microscope-(filter BV2A) with wavelengths in the range of 390–560 nm for tetracycline).

3. Results and discussion

Biomaterials science needs a proper understanding of the normal tissue repair mechanism for a rationale approach in developing an ideal bone substitute. The mechanical strength of bone results from the incorporation of mineral into the osteoid matrix template, and the factors that initiate the deposition of mineral in the calcification of bone are not well understood. Some authors have reported that the first phase that appears in the mineralization of extracellular matrix vesicles in the growth plates of long bone is amorphous calcium phosphate, while others report HA as the first phase (Wuthier and Evans 1975). Regardless of the above-mentioned hypothesis, the apatite of bone should be accepted as a living mineral since it undergoes continual growth, dissolution, and remodelling involving mineralization and resorption.

This study was focussed on synthesizing a bioactive calcium phosphate ceramic having the property of a reacting surface, keeping in mind the highly reactive physiological environment *in vivo*. Materials prepared by a sol–gel process are more bioactive than the materials of the same compositions prepared by other methods (Li and de Groot 1994). The surface of the granules were rough

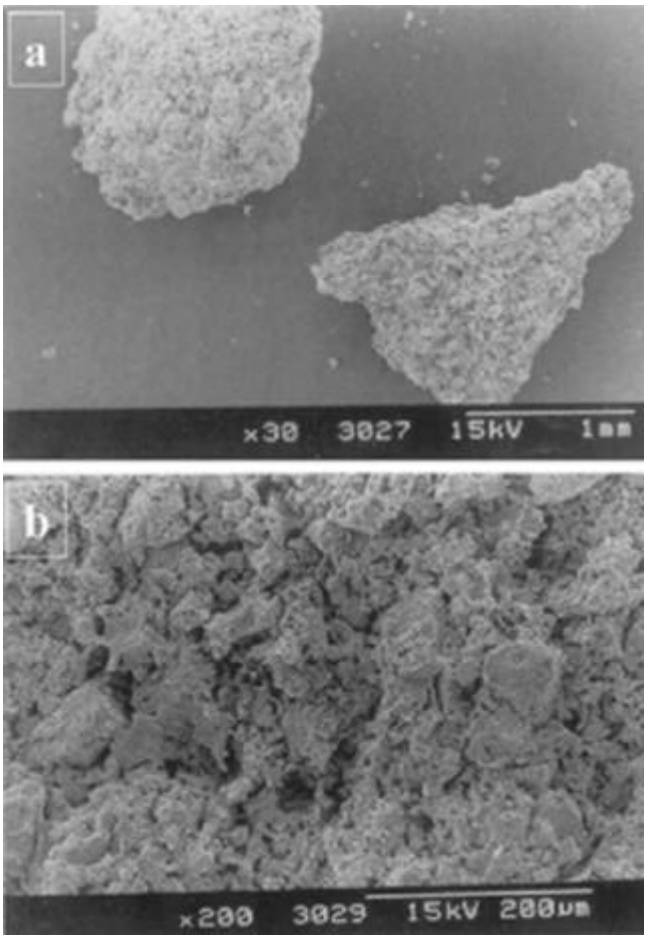

Figure 1. Scanning electron micrographs of **a.** bioactive glass–ceramic system (BGS) granules and **b.** magnified surface view of a single BGS granule.

and showed pores in the range of 10–50 μm and the granule size was in the range of 0·5–1 mm (figures 1a, b). The chemical reactions occurring on the ceramic surfaces play a significant role in the bone-bonding mechanism (van Blitterswijk *et al* 1985), because the crystal chemistry of the ceramic surface and the chemical constituents of the surrounding extracellular fluid in unison determines the nature of the solids to be formed on the surface of the material. X-ray diffraction of the BGS sintered granule powder revealed crystalline apatite [$Ca_{10}(PO_4)_6(OH)_2$] and wollastonite ($CaOSiO_2$) peaks (figure 2a). Role of apatite crystals is critical for bone formation as well as it is an inhibition for bone resorption too (Nesbitt and Horton 1997). It is also well known that proteins bind to the apatite crystal surface of the ceramic favouring secondary nucleation, thereby affecting the dissolution and re-precipitation process on the ceramic.

The FTIR spectrum showed the presence of the functional groups of phosphate in the material at 1117 cm^{-1}, 1051 cm^{-1}, 938 cm^{-1}, 581 cm^{-1}, 554 cm^{-1} and 429 cm^{-1} and the silicate peaks at 1022 cm^{-1}. The Si–O–Si stretch of the wollastonite was observed from 1117 to 716 cm^{-1} with minor peaks of P–O crystalline at 610–600 cm^{-1} and 569–559 cm^{-1}, P–O amorphous at 600–559 cm^{-1} and Si–O–Si bend at 554–425 cm^{-1} (figure 2b). The crystalline P–O could be due to the addition of P_2O_5 to the glass and was shown to eventually cause the amorphous calcium phosphate film to develop into a crystalline hydroxyapatite layer (Gross *et al* 1988). Certain hydroxyl groups such as SiOH and TiOH remaining in the sol–gel prepared materials are assumed to promote hydroxyapatite generation by providing sites for calcium phosphate nucleation (Li *et al* 1992). It is understood that biological mineralization generally incorporates both substitutions of CO_3^{2-} and HPO_4^{2-} into the apatite structure (Lacout 1992)—for hydroxyl ions (A type carbonated apatite) and for PO_4^{3-} groups (B type carbonated apatite).

The material seeded with the L929 fibroblast cells showed opening up of the grain boundaries, perhaps due to the leaching of the substantial concentration of soluble silica followed by calcium and phosphate ions from the material. This subsequently lead to dissolution, precipitation and crystallization of complex calcium phosphate precursor phases on the surface of the BGS disc in the cell culture medium (figure 3a). It has been reported that cell induced acidification also could lead to the dissolution of the calcium phosphate material (Evans *et al* 1984; Davies 1990).

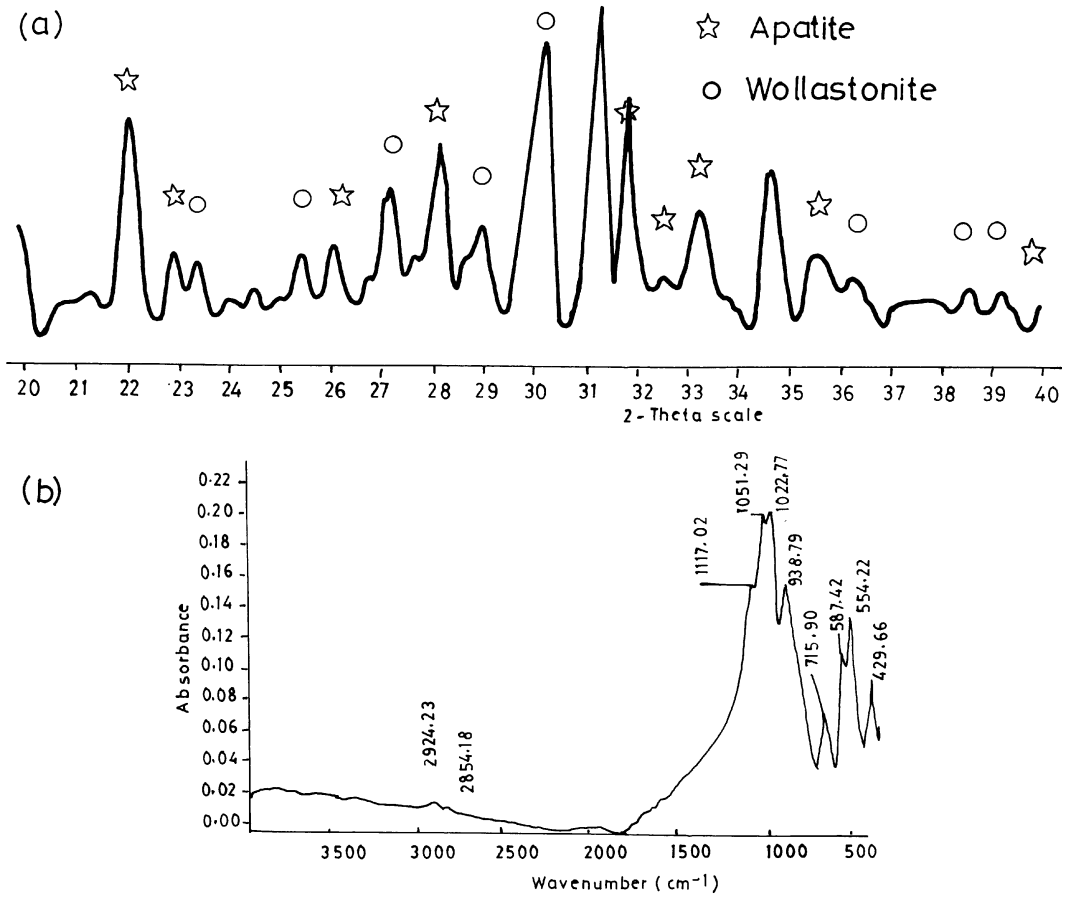

Figure 2. (**a**) X-ray diffraction pattern of bioactive glass–ceramic system (BGS) granules and (**b**) Fourier transform infrared spectrum of BGS granules.

The pH change on the material surface contributes prominently to cell attachment and the expression of cells depended on the preparation of the glass–ceramic surface and a better cellular response *in vitro* was achieved when the glass surface was less reactive (Vrouwenvelder *et al* 1992, 1994). Hence, the process of cell spreading is influenced by the nature of the underlying substrate as reported by Maroudas (1975). So in normal body fluid at pH 7·24, the material leaches initially *in vitro* due to its bioactive nature but becomes stable once the supersaturation is attained (Matsuda and Davies 1987). Li *et al* (1992) demonstrated that bone-like apatite layer is formed only after the formation of a silica gel layer in a CaO, SiO_2-based glasses prepared by the sol–gel method, when soaked in simulated body fluid at pH 7·4. BGS leaches rapidly at lower pH 3 to 5 and it is reported that pH of BGS surface remains high around 7·6 when in contact with the body fluids or in contact with the cells leading to less cell response on the material (Matsuda and Davies 1987). Hence, these possibilities of pH and its influence on surface change could be the reasons why only a small population of elongated fibroblast cells were seen adhered on the surface of the BGS material specifically noted more on the exposed regions of the grain boundaries of the disc (figure 3b). But this reduced cell attachment on the BGS does not mean toxicity to the cells, since the MTT assay in our study did not indicate a loss of cellular viability (80% viability) with the BGS extract and the adhered cells on the BGS disc surface showed no growth retardation, confirming that the material is biocompatible. Besides, BGS granules did not show any signs of toxicity embarrassment after 24 h in contact with L929 cells and even when maintained in culture for 6 days (data not shown). Cells spread centripetally from the granules to form a monolayer on the glass coverslip (figure 3c). Prior to immersion in the cell culture medium the surface of the BGS disc showed intact grain boundaries with the presence of macro cracks originating from the green compaction. However, after subjecting it to the culture medium, the material surface showed micropores, which may be due to the release of the calcium and phosphate ions from the material. It is also reported that pores present in pure silica, prepared by the sol–gel method, are nucleation sites for apatite (Pereira *et al* 1995). Therefore, the study of the surface morphology of the material is imperative to predict the changes involved prior to interfacial chemical bonding with the host tissue.

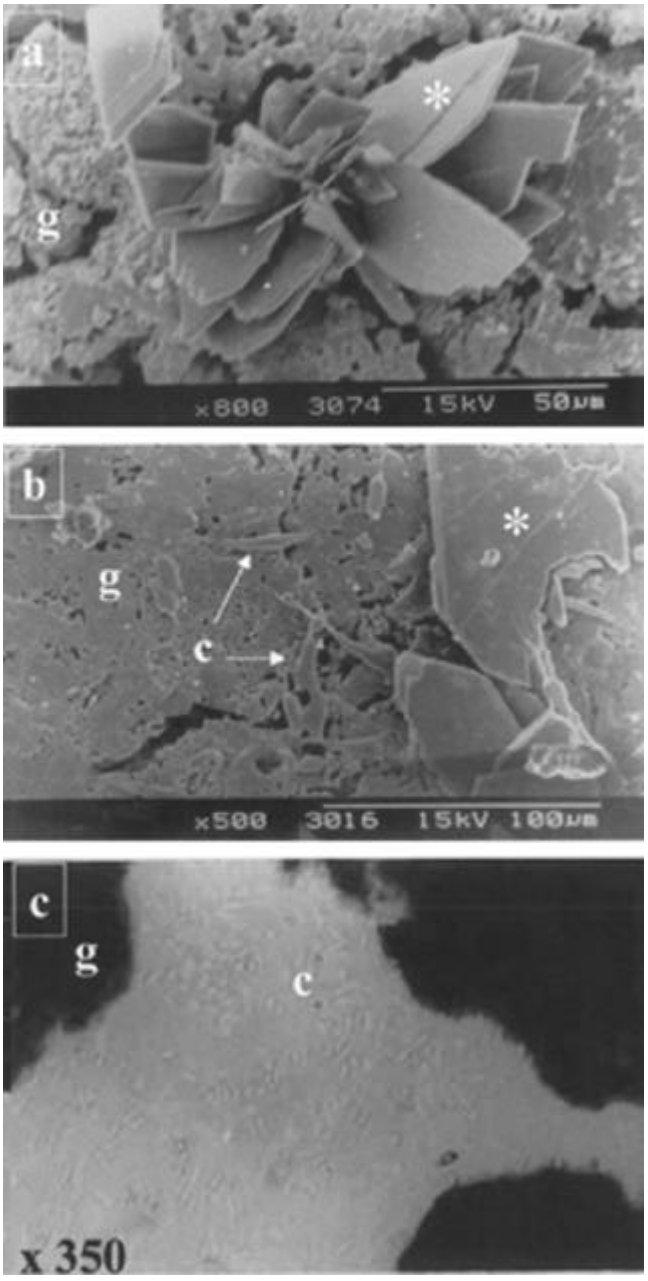

Figure 3. **a.** Scanning electron micrograph (SEM) of crystallization on bioactive glass–ceramic system (BGS) disc (48 h), **b.** SEM of L929 mouse fibroblast cells seeded on BGS disc (48 h) and **c.** photomicrograph of L929 mouse fibroblast cells in direct contact with the BGS granules (24 h), (original magnification: × 350; g = granules; c = cells; * = crystals).

For glasses with up to about 53 mole% of SiO_2, HCA crystallization occurs very rapidly on the glass surface within 2 h while glasses with SiO_2 content between 53 and 58 mole% of SiO_2 require two to three days to form both the amorphous calcium phosphate layer and to crystallize HCA. Compositions with > 60% SiO_2 do not form a crystalline HCA layer even after four weeks in SBF (Hench and LaTorre 1992). In short, the nature of the material (Klein *et al* 1990), the action of cells on the material (van der Meulen and Koerten 1994), the body fluids and pH (Matsuda and Davies 1987) influence dissolution of the material.

The rabbit as the experimental animal model was used on the basis of the cortical bone being Haversian and the stimulation of remodelling after injury is more similar to that of other larger mammals. The 2 mm defect made in

rabbit bone is the critical width for the tibia bone (Greiff 1978).

The BGS granules served as a template for maintaining cells in the defect and as a scaffold to guide bone morphogenesis (figure 4). Radiograph of the harvested tibia on explantation showed the material to be osteointegrated (figures 5a, b, c). Gross observation of the implant area did not show any inflammation or necrosis at all period of study.

When the animal was infused with Indian ink and barium sulphate, radiography did not reveal microcapillaries around the defect site. This does not mean that the implant area was not vascularized. However, after decalcifying the infused bone, feeble network of microcapillaries around the implant were observed in the radiograph under light microscopy (figure 6f).

Histologically, the osteogenesis was of intramembraneous type and no cartilage cells were observed at any

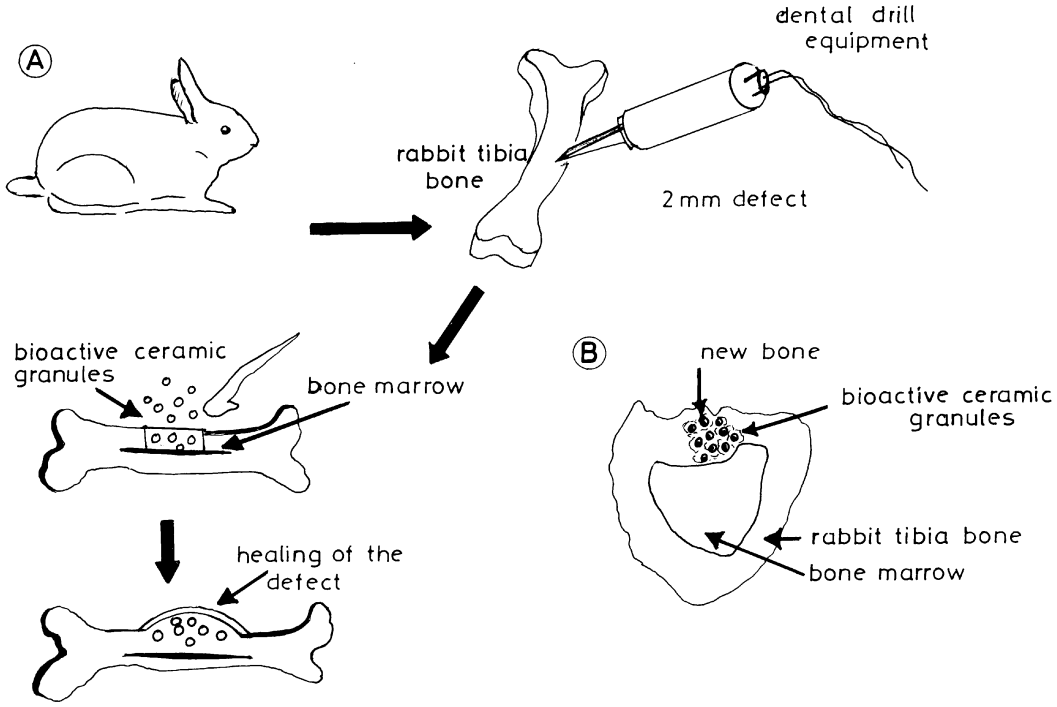

Figure 4. Schematic representation of (A) surgical procedure of implantation of bioactive glass–ceramic system (BGS) granules in rabbit tibia bone and (B) cross-section of tibia bone with implant granules.

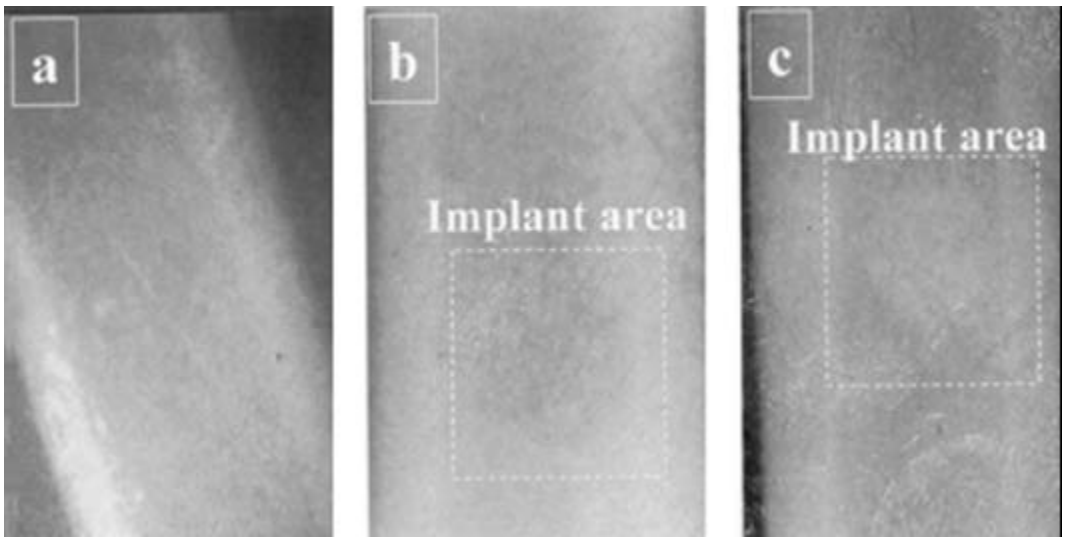

Figure 5. Radiographs of **a**. normal tibia bone, **b**. tibia bone with bioactive glass–ceramic system (BGS) granules, zero day and **c**. tibia bone with BGS granules, 12 weeks.

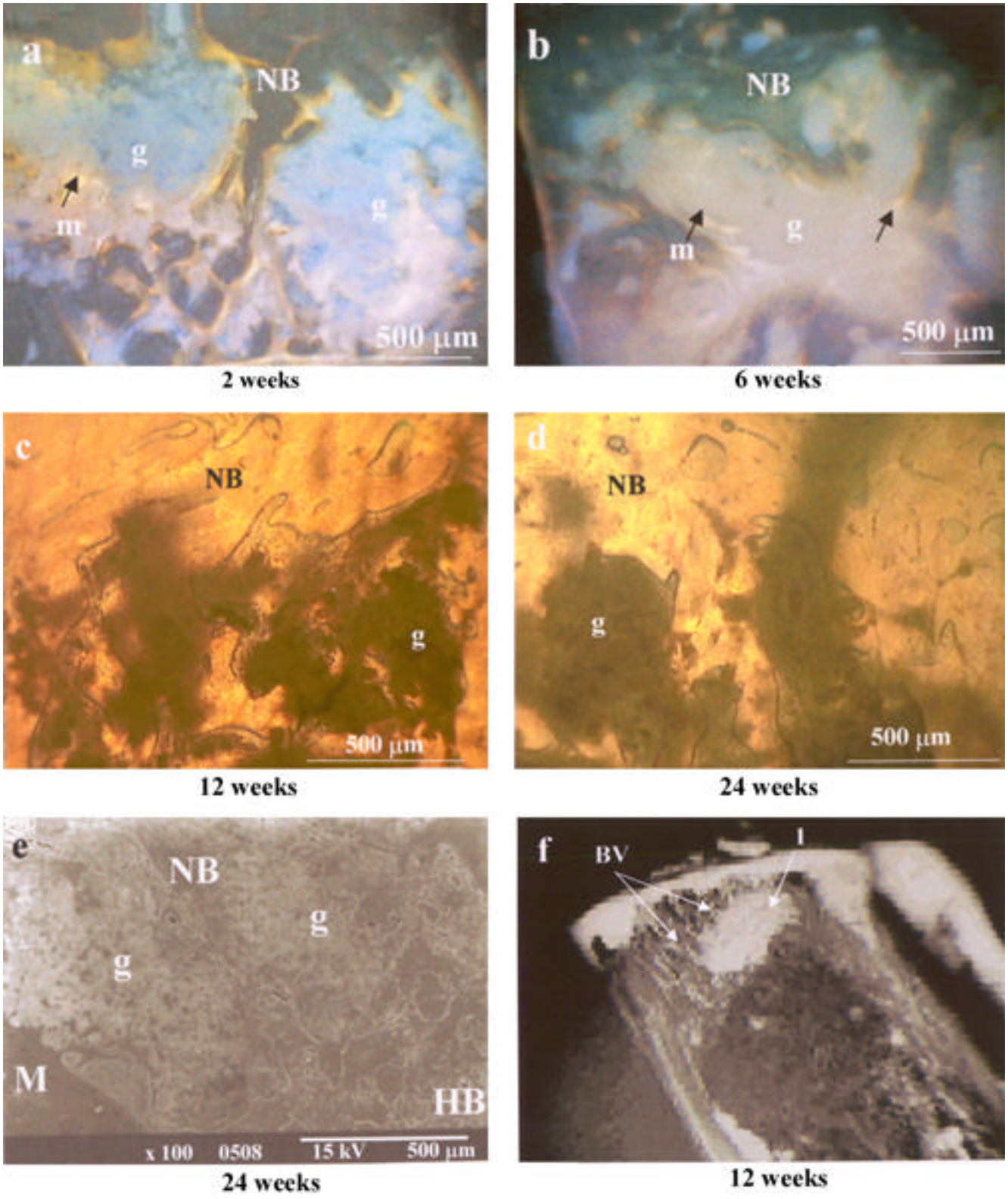

Figure 6. Fluorescence micrographs of unstained undecalcified polymethylmethacrylate (PMMA) cross sections of bioactive glass–ceramic system (BGS) granules in tibia bone at **a**. 2 weeks and **b**. 6 weeks. Mineralizing zones are shown by arrows. Photomicrographs of undecalcified PMMA cross sections of BGS granules in tibia bone stained with Stevenal's blue and counter stained with van Güson acid picrofuschin at **c**. 12 weeks and **d**. 24 weeks, **e**. scanning electron micrograph of unstained polished PMMA section of BGS granules implanted in bone for 24 weeks showing osteointegration and **f**. radiograph of decalcified PMMA unstained sections of BGS granules at 12 weeks in tibia bone showing the microcapillaries (NB = new bone; g = granule; m = mineralizing zones; M = bone marrow; bar = 500 µm; BV = blood vessels; I = implant).

period. Bone formation depends on the non-toxic surface that allows cell attachment and proliferation (Basle *et al* 1993). Trabecular bone formation was observed as early as 2 weeks in the interstices of the existing granules in close apposition to the BGS granules, without an intervening fibrous layer proving osteocompatibility and osteointegration. Osteointegration of the material with the host bone or the newly formed bone is a prerequisite for the implant success or failure. Morphologically, osseointegration is realized when there is direct contact of viable bone with the surface of the implant without an interposition of soft tissue at the light microscopical level (Boss 1999). Osteoblast-like cells, few macrophages and new microcapillaries were seen around the BGS granules. The granules had started cracking paving way for the invasion of the bony trabeculae within the cracks. The ability to bond to bone tissue is a unique property of bioactive ceramics and apatite formation is one of the key features in bone bonding. It has been reported that a surface apatite layer formed on AW–glass–ceramic as early as 7 days *in vitro* using pseudo extracellular fluid (Kokubo *et al* 1989, 1990) and also in *in vivo* 7 days after implantation in rat tibia (Neo *et al* 1993).

By 6 weeks, a network of woven bony trabeculae architecture with cellular infiltration was observed. The periosteal and the endosteal regions were completely closed, with new blood capillaries around the implant site. So the graft subsequently led to bone apposition on the granules and a complete bridging of the defect without fibrous tissue intervention. This observation was *in lieu* with the work of Ono *et al* (1990), where he reported that 89% of the AW–glass–ceramic surface was covered with new bone within 4 weeks of implantation in rat tibia. Active sites of bone mineralization in progress were evident by the presence of yellow fluorescence lines within the cracks and on the periphery of the granules as well as on the *de novo* bone in the vicinity of the ceramic granules. It was noted that bone formation progressed gradually from the margin of the defect cavity towards the granules and from the granules towards the host bone (figures 6a, b).

After 12 weeks, the mature woven bone had remodelled into lamellar bone in the periosteal and endosteal areas and the defect was completely healed. Whereas, in the mid cortical region the bone remained as immature woven bone (figure 6c). By 24 weeks, the mature woven bone was fully remodelled into lamellar bone in the periosteal, endosteal and cortical regions (figure 6d). Scanning electron microscopic observations also revealed good osteointegration with the BGS granules after 24 weeks (figure 6e) of implantation. The granules were observed intact even after 24 weeks, and are expected to be resorbed with time.

Quantitative histomorphometric analysis did not show any significant increase in new bone formation between 12 and 24 weeks (table 1). But qualitatively, a difference in the degree of bone maturation was observed, since by 24 weeks bone was fully remodelled into lamellar bone. Moreover, at 24 weeks, the surface area of the implant zone had increased due to implant degradation accompanied by bone remodeling, suggesting that the material degradation and bone formation had gone hand in hand at a faster pace from a very early period of 2–6 weeks. It was apparent that the BGS showed intramembraneous bone formation, which could be explained on the basis of osteoconduction, osteopromotion and osteoinduction via hematoma stabilization (Urist 1980; Whang *et al* 1999).

Larger the solubility rate of the ceramic, the more pronounced is the enhanced effect of bone tissue ingrowth (Ducheyne *et al* 1990; Ducheyne and Cuckler 1992; de Bruijn *et al* 1994). It has been reported that macrophages moved into the particles through these cracks and assisted in biodegradation (Schepers *et al* 1991; Schepers and Ducheyne 1997). Hench (1994) proposed that the soluble silicon activated stem cells producing TGF-*b* is reversibly adsorbed and desorbed in the hydrated silica calcium phosphate gel layers formed on the glass, which stimulates differentiation and subsequent growth of stem cells leading to rapid proliferation of bone in contact with bioactive glass particles.

The speed of formation of CO_3^{2-} apatite or biological apatite on the surfaces of bioactive materials *in vivo* controls the bone ingrowth rate and also new bone formation rate around the particles at a very early period (Oonishi *et al* 2000). Among bioactive ceramics, glass–ceramics containing apatite and wollastonite crystals have been found to have a high mechanical strength and showed newly formed apatite layer on their surfaces in the body environment (Nakamura *et al* 1985; Kitsugi *et al* 1987;

Table 1. Quantitative histomorphometric analyses of the area percentage of new bone and bone/implant in the rabbit tibial defect at 12 and 24 weeks (n = 3 sections).

	Implant zone (area %)		New bone zone (area %)	
Implanted material	3 Months	6 Months	3 Months	6 Months
Bioactive glass system–AW type (BGS)	32·51 ± 6·47	36·09 ± 8·35	67·77 ± 5·9	63·37 ± 8·57

Note: Implant zone = the whole defect area which encloses the new bone and implant granules; New bone zone = the area of new bone formed in the defect.

Kokubo *et al* 1990), similar to the apatite layer of natural bone where carbonate can substitute for phosphate, resulting in carbonate containing HA (Fourman *et al* 1972). Shors and Holmes (1993) had stated that an ideal bone graft substitute would mimic the natural bone and help in the stimulation of the osteoblast cells to differentiate and release the mineralizing matrix factors. In addition, size distributions of nanometer size pores of sol–gel derived bioactive glasses have a controlling effect in resorption and bone regeneration (Greenspan *et al* 1997; Wheeler *et al* 1997).

4. Conclusions

There is an increasing need for a suitable bone substitute as a stimulant for osteogenesis. Therefore, different types of bioactive ceramics individually or as composites can only compensate for various degenerating bone disorders like osteoporosis, periodontal disease, osteoarthritis, rheumatoid arthritis, bone cancer, avascular necrosis, and trauma. In this study, the bioactive glass system (BGS)–apatite wollastonite (AW) type granules synthesized by sol–gel route definitely enhanced the neo-osteogenesis process, and the healing of the defect was complete within 6 weeks after implantation. The BGS granules were seen well osteointegrated with newly formed bone and the host tissue as observed at 2, 6, 12 and 24 weeks postimplantation. By 24 weeks the size of the granules reduced in concert with bone formation. BGS proved to be an effective osteostimulator and osteoconductor and shows promise as a bioactive, biodegradable bone graft material. It also warrants further investigation in large defects in species other than rabbit, considering the potential clinical relevance of these findings.

The future optimizations of these bioactive materials will be combined with impregnation of cells and growth factors for successful surgical outcomes. Modifying or optimizing the compositions of the bioactive glass offers great promise in bioceramic engineering for producing a new generation of biomaterials for bone tissue engineering to restore or replace lost, diseased or congenitally missing bone.

Acknowledgements

Financial assistance from DST (SP/SO/B68/95), New Delhi, is gratefully acknowledged. The Director SCTIMST, for the facilities provided to carry out this work, Dr R Sivakumar (former Head, BMT, SCTIMST) for the technical guidance during this work, Dr Arthur Vijyan Lal, SCTIMST, for the microradiographic studies, R Sreekumar, SCTIMST, for the scanning electron micrographs, C Radhakumary, SCTIMST, for the FTIR spectrum and Dr Mira Mohanty, SCTIMST, for her valuable suggestions during this work, are all thankfully acknowledged.

References

ASTM: American Society for Testing of Materials, West Conshohocken, PA, Standard F981-91, Standard practice for assessment of compatibility for surgical implants with respect to effect of materials on muscle and bone

Basle M F, Rebel A, Grizon F, Daculsi G, Passuti N and Filmon R 1993 *J. Mater. Sci. Mater. Med.* **4** 273

Boss J H 1999 *J. Long-term Effects of Medical Implants* **9** 1

Bruder S P, Kurth A A, Shea M and Hayes W C 1998 *J. Orthop. Res.* **16** 155

Davies J E 1990 *Handbook of bioactive ceramics* (eds) J Wilson-Hench (Boca Raton: CRC Press) **1** 195

de Bruijn J D, Bovell Y P and van Blitterswijk C A 1994 *Biomaterials* **15** 543

Ducheyne P and Cuckler J 1992 *Clin. Orthop. Rel. Res.* **276** 102

Ducheyne P, Beight J, Cuckler J, Evans B and Radin S 1990 *Biomaterials* **11** 531

Epstein N 1989 *Smithsonian* 509

Evans R W, Cheung H S and McCarty D J 1984 *Calcified Tissue International* **36** 645

Fourman P P, Levell R J and Morgan D B 1972 *Calcium metabolism and the bone* (Philadelphia: F A Davies Co.) p. 3

Greenspan D C, Zhong J P, LaTorre G P and Booher M 1997 The *in vitro* degradability of sol–gel bioglass®, in *Transactions of the 23rd annual meeting of the society for biomaterials* (New Orleans, LA)

Greiff J 1978 *Injury* **10** 257

Gross U, Raimund Kinne, Hermann-Josef Schmitz and Volker Strunz 1988 *The response of bone to surface-active glasses/glass–ceramics*, in *CRC critical reviews in biocompatibility* (ed.) Larry L Hench (Boca Raton: CRC Press) Vol. 4, pp 155–180

Gurr E 1973 *Biological staining methods* (Buckinghamshire, England: Searle Diagnostic Gurr Products) 8th ed., p. 111

Hench L L 1988 *Ann. NY Acad. Sci.* **523** 54

Hench L L 1991a *J. Am. Ceram. Soc.* **74** 1487

Hench L L 1991b *The bone–biomaterial interface* (ed.) J E Davies (Toronto, Canada: University of Toronto Press) p. 33

Hench L L 1994 *Bioactive ceramics: Theory and clinical applications in bioceramics* (eds) O H Anderson and A Yli-Urpo (Oxford, England: Butterworth-Heinemann Ltd.) p. 3

Hench L L and Clark A E 1981 *Fundamental aspects of biocompatibility* (ed.) D F Williams (Boca Raton, FL: CRC Press) **1** p. 67

Hench L L and West J K 1996 *Life Chem. Rep.* **13** 187

Hench L L and Wilson J 1984 *Science* **226** 630

Hench L L and Andersson O 1993 *Introduction to bioceramics* (*Advanced Series in Ceramics* – vol. 1) (eds) L L Hench and J Wilson (Singapore, New Jersey: World Scientific Publishing Co. Pvt. Ltd.) **3** p. 41

Hench L L and Paschall H A 1973 *J. Biomed. Mater. Res.* **4** 25

Hench L L and LaTorre G P 1992 *Reaction kinetics of bioactive ceramics Part IV: Effect of glass and solution composition*, in *Bioceramics 5* (eds) T Yamamuro, T Kokubo and T Nakamura (Kyoto, Japan: Kobonshi Kankokai Inc.) pp 67–74

Holmes R E, Wandrop R W and Wolford L M 1988 *J. Oral Maxillofac. Surg.* **46** 661

Hupp J R and McKenna S J 1988 *J. Oral Maxillofac. Surg.* **46** 538
Kitsugi T, Nakamura T, Yamamuro T, Kokubo T, Shibuya T and Takagi M 1987 *J. Biomed. Mater. Res.* **21** 1255
Kitsugi T, Yamamuro T, Nakamura T and Oka M 1995 *Biomaterials* **16** 1101
Klein C P, de Blieck-Hogervorst J M, Wolke J G and de Groot K 1990 *Biomaterials* **11** 509
Kokubo T, Kushitani H, Ebisawa Y, Kitsuji T, Kotani S, Ouro K and Yamamuro T 1989 *Bioceramics* (eds) H Oonishi, H Aoki and K Sawai (Tokyo: Ishiyaku Euro America) **1** p. 157
Kokubo T, Kushitani H, Sakka S, Kitsugi T and Yamamuro T 1990 *J. Biomed. Mater. Res.* **24** 721
Lacout J L 1992 *Biomaterials—Hard tissue repair and replacement* (ed.) D Muster (Amsterdam, The Netherlands: Elsevier Science Publishers BV) p. 81
Li P and de Groot K 1994 *J. Sol-Gel Sci. Technol.* **12** 155
Li P, Ohtsuki C, Kokubo T, Nakasihi K, Suga N, Kawamura T and Yamamuro T 1992 *J. Am. Ceram. Soc.* **75** 2094
Ludwigson D C 1964 *J. Metals* **16** 1
Maroudas N G 1975 *J. Theor. Biol.* **49** 417
Matsuda T and Davies J E 1987 *Biomaterials* **8** 275
Nakamura T, Yamamuro T, Higashi S, Kokubo T and Ito S 1985 *J. Biomed. Mater. Res.* **19** 685
Neo M, Nakamura T, Ohtsuki C, Kokubo T and Yamamuro T 1993 *J. Biomed. Mater. Res.* **27** 999
Nesbitt S A and Horton M A 1997 *Science* **276** 266
Ono K, Yamamuro T and Nakamura T 1990 *Biomaterials* **11** 265
Oonishi H *et al* 2000 *J. Biomed. Mater. Res.* **51** 37
Ohtsuki C, Kushitani H, Kokubo T, Kotani S, Yamamuro T and Nakamura T 1991 *J. Biomed. Mater. Res.* **25** 1363
Pereira M M, Clark A E and Hench L L 1995 *J. Am. Ceram. Soc.* **78** 2463
Plenk H 1986 in *Techniques of biocompatibility testing* (*CRC series in biocompatibility*) (ed.) D F Williams (Boca Raton, Florida: CRC Press Inc.) **vol. 1**, p. 35
Ratner B D, Hoffman A S, Schoen F J and Lemons J E (eds) 1996 *Biomaterial science: An introduction to materials in medicine* (New York: Academic Press)
Schepers E and Ducheyne P 1997 *J. Oral Rehab.* **24** 171
Schepers E, deClercq M, Ducheyne P and Kempeneers R 1991 *J. Oral Rehab.* **18** 439
Shors E C and Holmes R E 1993 in *An introduction to bioceramics, advanced series in ceramics* (eds) L L Hench and J Wilson (Singapore: World Scientific) **1** p. 181
Urist M R 1980 *Fundamental and clinical bone physiology* (ed.) M R Urist (Philadelphia: Lippincott) p. 331
Van Blitterswijk C A, Grote J J, Kruypers W, Blok Van Hoek C J G and Deams W T 1985 *Biomaterials* **6** 243
Van der Meulen J and Koerten H K 1994 *J. Biomed. Mater. Res.* **28** 1455
Vrouwenvelder W C A, Groot C G and de Groot K 1992 *Biomaterials* **13** 382
Vrouwenvelder W C A, Groot C G and de Groot K 1994 *Biomaterials* **15** 97
Whang K *et al* 1999 *Tissue Eng.* **5** 35
Wheeler D L, Stokes K E, Park H M and Hollinger J O 1997 *J. Biomed. Mater. Res.* **35** 249
Wilson J and Low S J 1992 *J. Appl. Biomater.* **3** 123
Wuthier A and Evans E 1975 *Calcif. Tissue Res.* **19** 197